Big Bang Nucleosynthesis

Big Bang Kernesyntese

Hans Brüner Dein
201706079

Master's Thesis in Cosmology
February 2024

Supervisor: Thomas Tram

Department of Physics and Astronomy
Aarhus University

Colophon

Big Bang Nucleosynthesis

— Big Bang Kernesyntese

Master's thesis by Hans. Written under supervision by Asc.Prof. Thomas Tram, Department of Physics and Astronomy, Aarhus University.

Typeset by the author with LaTeX and the memoir document class, using Linux Libertine and Linux Biolinum 11.0/13.6pt.

Printed at Aarhus University

Abstract (English)

Nucleosyntehesis is wack

Resumé (Dansk)

Kernesyntese er spøjs

Preface

This thesis concludes my Master's degree in/at .....

Contents

Introduction

This thesis is about nucleosynthesis

A brief history of early nucleosynthesis

A second after the Big Bang, the universe is at 10^10K. Though quite hot, this temperature is low enough that neutrons and protons can no longer maintain thermodynamics equilibrium, freezing their ratio at one to five. At approximately 200 seconds the universe has cooled sufficiently so that high energy photons can no longer destroy deuterium. This causes almost all neutrons to be use in the creation of deuterium, which is rapidly converted to helium. Due to the delay caused by deuterium, the temperature and density of the universe will be to low to create any more than trace amounts of heavier elements. And so a few minutes after it began, primordial nucleosynthesis ends. Barring radioactive decay, the abundance of the various elements will remain unchanged, until the first star appear 10^8 years later.

Chapter 1

BBN physics and cosmology

To understand the process of Big Bang nucleosynthesis, we must examine the intersection between Cosmology, thermodynamics, particle, and nuclear physics. Though this might seem daunting, it turns out that the unique conditions during this epoch allow for extensive simplifications of this otherwise monumental task. Throughout this section we use $\hbar = c = k_B = 1$.

1.1 Determining background parameters

1.1.1 Temperature and scale factor

BBN takes place after inflation while the universe is still radiation dominated. This can be described by the Friedman equation, which can be further simplified with the reasonable approximation, that both curvature and the cosmological constant are zero.

$$H^2 = \left(\frac{\dot{a}}{a}\right)^2 = \frac{8\pi G}{3}\rho_{tot}, \tag{1.1}$$

with ρ_{tot} referring to the total energy density of photons, leptons and baryons,

$$\rho_{tot} = \rho_\gamma + \rho_\nu + (\rho_{e^-} + \rho_{e^+}) + \rho_b. \tag{1.2}$$

(1.1) can be rearranged as a differential equation explicitly describing the time evolution of the scale factor.

$$\frac{da}{dt} = a\sqrt{\frac{8\pi G}{3}\rho_{tot}(T, a)} \tag{1.3}$$

To find an expression for the temperature evolution, we utilize energy conservation. We can consider the neutrinos as decoupled during BBN, and so the photon temperature will be determined by the remaining components. Since this point the universe is very much homogeneous and isotropic, we utilize the fluid equation for adiabatic expansion [9, (4.44)].

$$\dot{\rho_{set}} + 3\frac{\dot{a}}{a}(\rho_{set} + P_{set}) = 0 \tag{1.4}$$

With ρ_{set} being the density of none-decoupled components and P_{set} being their pressures.

$$\rho_{set} = \rho_\gamma + (\rho_{e^-} + \rho_{e^+}) + \rho_b \quad , \quad P_{set} = P_\gamma + (P_{e^-} + P_{e^+}) + P_b \tag{1.5}$$

Using the chain rule we can then set up a differential equation describing the time evolution of the photon temperature.

$$\frac{dT}{dt} = -3\frac{\dot{a}}{a}\frac{\rho_{set}(T,a) + P_{set}(T,a)}{\frac{d\rho_{set}(T,a)}{dT}} \tag{1.6}$$

1.1.2 Additional parameters

Most BBN codes are based on the original code by Wagoner described in section 2.1. These don't track the scale factor, but instead use the quantity h.

$$h = M_u \frac{n_b}{T_9^3} \tag{1.7}$$

M_u being atomic mass units, n_b the baryon number density, and T_9 the temperature in 10^9 Kelvin. This quantity was useful since it stays approximately constant throughout BBN, while being easy to directly convert to baryon density. However, with modern computers this numerical simplicity is inconsequential, and as such it is more instructive to track the scale factor. The electron chemical potential was also tracked by the Wagoner code and its successors. The main effect of this is ensuring a non-zero electron density after e^- e^+ annihilation. We can easily set this to 0, as the impact will be 3 orders of magnitude lower than the already miniscule impact of the baryon density.

Neutrino temperature?

1.2 Energy densities and pressure

In the very early universe most particles were in thermal equilibrium, and can be described by the rules of statistical physics. The average number of particles in a given state is governed by the Fermi-Dirac distribution for fermions, and the Bose-Einstein distribution for bosons.

$$\bar{n}_{FD} = \frac{1}{e^{(E-\mu)/T} + 1} \quad , \quad \bar{n}_{BE} = \frac{1}{e^{(E-\mu)/T} - 1} \tag{1.8}$$

With E being the total energy each particle in the state and μ the chemical potential. The number density can be found generally by integrating over all possible momentum states.

$$n(T) = \frac{g}{(2\pi)^3}\int_0^\infty \bar{n}(p,T)dp^3 = \frac{g}{2\pi^2}\int_0^\infty \bar{n}(p,T)p^2dp \tag{1.9}$$

With g being the degeneracy parameter. We can similarly find an expression for the energy density by multiplying the integrand by the relativistic energy $E^2 = m^2 + p^2$.

$$\rho(T) = \frac{g}{2\pi^2}\int_0^\infty \bar{n}(p,T)\sqrt{m^2+p^2}p^2dp \tag{1.10}$$

Pressure is defined as the force exerted per unit area. Consider a relativistic particle confined to a sphere of radius r. Whenever it collides with the surface, it will exert a force proportional to the change in momentum.

$$F = \frac{dp}{dt} = \frac{\Delta p}{\Delta t} \quad , \quad \Delta p = 2p\cos\theta, \tag{1.11}$$

with θ being the incident angle.

The time between collisions can be deduced based on the distance traveled.

$$\Delta t = \frac{L}{\mathrm{v}} = L\frac{\sqrt{m^2+p^2}}{p}, \tag{1.12}$$

with distance between collisions L and velocity v.

Next, consider the triangle created by the center of the sphere and two consecutive collision points. Using the law of cosines we can determine L.

$$r^2 = L^2 + r^2 + 2Lr\cos\theta \Rightarrow L = 2r\cos\theta \tag{1.13}$$

We can then determine the force and pressure exerted on the sphere by each particle.

$$F = \frac{p^2}{r\sqrt{m^2+p^2}} \quad , \quad P = \frac{p^2}{4\pi r^3\sqrt{m^2+p^2}} \tag{1.14}$$

Generalizing this for any volume, we get the integral for the total pressure of a relativistic gas.

$$PV = \frac{p^2}{3\sqrt{m^2+p^2}} \tag{1.15}$$

$$P(T) = \frac{g}{6\pi^2}\int_0^\infty \bar{n}(p,T)\frac{p^4}{\sqrt{m^2+p^2}}dp \tag{1.16}$$

Additionally, we see that the pressure of an ultra-relativistic gas follows a simple relation.

$$P(T) = \frac{\rho(T)}{3} \quad (\text{for } m \ll p) \tag{1.17}$$

1.2.1 Photons

Photons are massless bosons with 2 distinct polarizations for each momentum state. With $g = 2$, we use 1.10 to determine the energy density.

$$\rho_\gamma(T) = \int_0^\infty \frac{p^3}{\pi^2}\frac{1}{e^{p/T}-1}dp = \frac{T^4}{\pi^2}\int_0^\infty \frac{u^3}{e^u-1}du \tag{1.18}$$

This integral is a well know representation of the Riemann Zeta function [19, (25.5.1)].

$$\rho_\gamma(T) = \frac{T^4}{\pi^2}\Gamma(4)\zeta(4) = \frac{\pi^2}{15}T^4 \tag{1.19}$$

From this we can easily determine the temperature derivative and pressure.

$$\frac{d\rho_\gamma(T)}{dT} = \frac{4}{15}\pi^2T^3 \quad , \quad P_\gamma(T) = \frac{\rho_\gamma(T)}{3} \tag{1.20}$$

1.2.2 Neutrinos

For neutrinos $g = 2N_\nu$, to account for the different species and their antiparticles.

$$\rho_\nu(T_\nu) = N_\nu \int_0^\infty \frac{p^3}{\pi^2} \frac{1}{e^{p/T_\nu} + 1} dp = N_\nu \frac{T_\nu^4}{\pi^2} \int_0^\infty \frac{u^3}{e^u + 1} du \tag{1.21}$$

This is also an integral representation of the Riemann Zeta function [19, (25.5.3)].

$$\rho_\nu(T_\nu) = N_\nu \frac{T_\nu^4}{\pi^2} \Gamma(4)\zeta(4)(1 - 2^3) = N_\nu \frac{7}{8} \frac{\pi^2}{15} T_\nu^4 \tag{1.22}$$

The effective neutrino number is $N_\nu = 3.045$ to take into account the non-instantaneous decoupling of the neutrinos as well as QED plasma effects [12].

Tracking the neutrino temperature separately is quite troublesome, luckily we don't have to. Since neutrinos decouple very early, the only significant change in their energy density will be due to the expansion of the universe. Therefore, we can track the later evolution using the scale factor.

$$\rho_\nu(t) = \frac{\rho_\nu(T_i)}{a(t)^4} \tag{1.23}$$

1.2.3 Electrons and positrons

Electrons and positrons unfortunately have mass, which makes solving for their density and pressure much more troublesome.

$$\rho_\pm(T) = \frac{1}{\pi^2} \int_0^\infty \frac{\sqrt{m^2 + p^2}}{e^{(E \pm \mu)/T} + 1} p^2 dp \tag{1.24}$$

$$P_\pm(T) = \frac{1}{3\pi^2} \int_0^\infty \frac{1}{e^{(E \pm \mu)/T} + 1} \frac{p^4}{\sqrt{m^2 + p^2}} dp \tag{1.25}$$

Inspired by the derivation of Chandrasekhar [1], we will solve these integrals by using the rapidity θ.

$$\sinh\theta = \frac{p}{m} \quad , \quad \cosh\theta = \frac{E}{m} \tag{1.26}$$

After a simple change of variable we get a much nicer form of the integrals.

$$\rho_\pm(T) = \frac{m^4}{\pi^2} \int_0^\infty \frac{\sinh^2\theta \cosh^2\theta}{e^{(m\cosh\theta \pm \mu)/T} + 1} d\theta \tag{1.27}$$

$$P_\pm(T) = \frac{m^4}{3\pi^2} \int_0^\infty \frac{\sinh^4\theta}{e^{(m\cosh\theta \pm \mu)/T} + 1} d\theta \tag{1.28}$$

Before and during BBN $(E \pm \mu)/T$ will be strictly positive, and we can therefore perform a series expansion, which converges nicely for high temperatures.

$$\frac{1}{e^{(m\cosh\theta \pm \mu)/T} + 1} = \sum_{n=1}^{n=\infty} (-1)^{n+1} e^{-n\frac{m}{T}\cosh\theta} e^{\mp n\frac{\mu}{T}} \tag{1.29}$$

The chemical potential does not depend on the rapidity, allowing us to get combined pressure of both electrons and positrons.

$$P_e(T) = P_- + P_+ = \frac{2m^4}{3\pi^2}\sum_{n=1}^{n=\infty}(-1)^{n+1}\cosh\left(n\frac{\mu}{T}\right)\int_0^\infty e^{-n\frac{m}{T}\cosh\theta}\sinh^4\theta d\theta \tag{1.30}$$

These terms are integral representations of modified Bessel functions [19, (10.32.8)].

$$\int_0^\infty e^{-z\cosh\theta}\sinh^4\theta d\theta = 4\frac{\Gamma(2+\frac{1}{2})}{\sqrt{\pi}z^2}K_2(z) = 3z^{-2}K_2(z) \tag{1.31}$$

With $z = n\frac{m}{T}$, we can get the total pressure expressed as a sum of modified Bessel functions.

$$P_e(T) = \frac{2m^2}{\pi^2}T^2\sum_{n=1}^{n=\infty}\frac{(-1)^{n+1}}{n^2}\cosh\left(n\frac{\mu}{T}\right)K_2\left(n\frac{m}{T}\right) \tag{1.32}$$

The energy density can be found by the same way, by first utilizing the identity $cosh^2 = sinh^2 + 1$, to get the energy density in terms of $\sinh\theta$.

$$\rho_e(T) = \rho_- + \rho_+ = \frac{2m^4}{\pi^2}\sum_{n=1}^{n=\infty}(-1)^{n+1}\cosh\left(n\frac{\mu}{T}\right)\int_0^\infty e^{-n\frac{m}{T}\cosh\theta}\left(\sinh^4\theta + \sinh^2\theta\right)d\theta \tag{1.33}$$

The $\sinh^4$ term is clearly the same as for the pressure up to a factor of 3. Comparing this to the results for massless particles, this term can be interpreted as the thermal energy of the electron gas. The second term also corresponds to a modified Bessel function, though of first rather than second order [19, (10.32.8)]. Combined this grants us the sum describing the total energy density of electrons and positrons.

$$\rho_e(T) = \frac{2m^2}{\pi^2}T^2\sum_{n=1}^{n=\infty}\frac{(-1)^{n+1}}{n^2}\cosh\left(n\frac{\mu}{T}\right)\left(3K_2\left(n\frac{m}{T}\right) + n\frac{m}{T}K_1\left(n\frac{m}{T}\right)\right) \tag{1.34}$$

Using recursion relations for the modified Bessel functions [19, (10.29.1)], we see that this is equivalent to the expression used in other BBN codes [7].

$$3K_2(z) + zK_1(z) = 3\frac{z}{4}[K_3(z) - K_1(z)] + zK_1(z) = \frac{z}{4}[3K_3(z) + K_1(z)] \tag{1.35}$$

$$\rho_e(T) = \frac{m^3}{2\pi^2}T\sum_{n=1}^{n=\infty}\frac{(-1)^{n+1}}{n}\cosh\left(n\frac{\mu}{T}\right)\left(3K_3\left(n\frac{m}{T}\right) + K_1\left(n\frac{m}{T}\right)\right) \tag{1.36}$$

As mentioned many older BBN codes track the parameter $\phi_e = \frac{\mu}{T}$, but this is unnecessary, as the electron density after e^- e^+ annihilation is 3 orders of magnitude lower than the already negligible contribution of the baryons. So for the remaining calculation we set $\mu = 0$.

Finding the temperature derivative of the electron energy density, can also be achieved using the recursion relations for Bessel functions [19, (10.29.2)].

$$\frac{d}{dz}\frac{1}{z}[3K_3(z)+K_1(z)] = -3[z^{-2}K_3(z)+z^{-1}K_2(z)+3z^{-2}K_3(z)]-z^{-1}K_2 \tag{1.37}$$

$$= -12z^{-2}K_3(z)-4z^{-1}K_2(z) \tag{1.38}$$

$$= -\frac{1}{z}[2K_4(z)-2K_2(z)+4K_2(z)] \tag{1.39}$$

$$= -\frac{2}{z}[K_4(z)+K_2(z)] \tag{1.40}$$

With this it is easy to determine the temperature derivative.

$$\frac{d\rho_e(T)}{dz} = -\frac{m^3}{\pi^2}T\sum_{n=1}^{n=\infty}\frac{(-1)^{n+1}}{n}\left(K_4\left(n\frac{m}{T}\right)+K_2\left(n\frac{m}{T}\right)\right) \tag{1.41}$$

$$\frac{d\rho_e(T)}{dT} = \frac{m^4}{\pi^2}\frac{1}{T}\sum_{n=1}^{n=\infty}(-1)^{n+1}\left(K_4\left(n\frac{m}{T}\right)+K_2\left(n\frac{m}{T}\right)\right) \tag{1.42}$$

1.2.4 Baryons

The temperatures at which BBN takes place are too low for Baryon pair production. Therefore, the number density of baryons can be solely determined by the scale factor and some known density.

$$n_b(a) = \frac{a_0^3}{a^3}n_b(a_0) \tag{1.43}$$

To determine baryon density $n_b(a_0)$, we use the baryon photon/ratio η.

$$n_b = n_\gamma(T)\eta \quad , \quad n_\gamma(T) = \frac{T^3}{\pi^2}\Gamma(3)\zeta(3) \tag{1.44}$$

From the CMB we can measure the value of η, during recombination, but unlike baryons the number of photons does not remain unchanged from the start of BBN until recombination. The only significant source of photons is the annihilation of the electron-positron pairs. We can account for this using conservation of entropy. For a given species we define the entropy density [8, (3.91)].

$$s = \frac{\rho+P}{T} \tag{1.45}$$

Setting $a = 1$ at the start of our BBN calculations, we get a relation between the total entropy before and after annihilation.

$$s_\gamma(T_{CMB})a_{CMB}^3 = s_e(T_i)+s_\gamma(T_i) \tag{1.46}$$

The photon number density is directly proportional to entropy density, both scaling with T^3. This allows us to restate (1.46) only in terms of the initial entropy density.

$$n_\gamma(T_{CMB})a_{CMB}^3 = \frac{n_\gamma(T_i)}{s_\gamma(T_i)}\left(s_e(T_i)+s_\gamma(T_i)\right) \tag{1.47}$$

From this we get the baryon density as a function of the initial photon and electron density and pressure.

$$n_b(a_{CMB})a_{CMB}^3 = n_\gamma(T_i)\left(\frac{s_e(T_i)+s_\gamma(T_i)}{s_\gamma(T_i)}\right)\eta \tag{1.48}$$

$$n_b(a) = \frac{1}{a^3}n_\gamma(T_i)\left(1+\frac{\rho_e(T_i)+P_e(T_i)}{\rho_\gamma(T_i)+P_\gamma(T_i)}\right)\eta \tag{1.49}$$

With T_i being the initial temperature. Finally, to get the energy density we simply need to sum over all different nuclei.

$$\rho_b(a) = n_b(a)\sum_i Y_i m_i \tag{1.50}$$

For each isotope m_i is the mass, and Y_i is the ratio between the number of nuclei and the total number of nucleons. Y_i is often defined as $Y_i = X_i/A_i$, with X_i being the mass fraction, and A_i the atomic weight [5]. The difference in per nucleon mass of different isotopes, causes these two definitions to have a relative difference of $1e-5$, which can be safely neglected. Furthermore, since eta is only known with an accuracy of 1% [15], we can approximate that all baryons have the same mass as a lone proton reducing (1.50) to $\rho_b(a) \approx n_b(a)m_p$.

The baryon pressure can be found using the ideal gas law.

$$P_b(a) = n_b(a)T\sum_i Y_i \tag{1.51}$$

Unlike for the relativistic particles, the baryon pressure is several orders of magnitude lower than the density. Since the baryon density is already comparatively low, the pressure will be completely negligible.

1.3 Nuclear reactions

All relevant nuclear reactions involve at most 6 different nuclei. Generally we can write these reactions as

$$N_iX_i + N_jX_j + N_kX_k \leftrightharpoons N_nX_n + N_mX_m + N_lX_l, \tag{1.52}$$

where N_i is the number of nuclei X_i, that enter the reaction. The change in abundance Y_i of any nuclei is given by the sum of all reactions that create or destroy it.

$$\frac{dY_i}{dt} = \sum_{\lambda_i}\frac{N_i}{n_b}\left(\lambda_{nml\to ijk}\frac{Y_n^{N_n}Y_m^{N_m}Y_l^{N_l}}{N_n!N_m!N_l!}n_b^{(N_n+N_m+N_l)} - \lambda_{ijk\to nml}\frac{Y_i^{N_i}Y_j^{N_j}Y_l^{N_k}}{N_i!N_j!N_k!}n_b^{(N_i+N_j+N_k)}\right) \tag{1.53}$$

With λ being the reaction rate, and n_b the baryon number density. The reaction rate $\lambda(T)$ only depends on the kinetic energy of the baryons and by extension the photon temperature. $n_b(a)$ only depends on the scale factor as shown in (1.49).

From (1.53) we can quite easily determine the partial derivatives required for the construction of a Jacobian.

$$\frac{\partial}{\partial Y_j}\frac{dY_i}{dt} = -\sum_{\lambda_{ij\to}} N_i N_j \lambda_{ijk\to nml} \frac{Y_i^{N_i} Y_j^{N_j-1} Y_l^{N_k}}{N_i! N_j! N_k!} n_b^{(N_i+N_j+N_k-1)} \tag{1.54}$$

$$\frac{\partial}{\partial Y_n}\frac{dY_i}{dt} = \sum_{\lambda_{n\to i}} N_i N_n \lambda_{nml\to ijk} \frac{Y_n^{N_n-1} Y_m^{N_m} Y_l^{N_l}}{N_n! N_m! N_l!} n_b^{(N_n+N_m+N_l-1)} \tag{1.55}$$

1.3.1 Proton ⇋ neutron rate

At $T > 10^{10}$K any created nuclei will be instantly destroyed by high energy photons. This leaves only the conversion between neutrons and positrons, which is governed by the following reactions

$$n \leftrightarrow p + e^- + \bar{\nu}_e \tag{1.56}$$

$$n + e^+ \leftrightarrow p + \bar{\nu}_e \tag{1.57}$$

$$n + \nu_e \leftrightarrow p + e^- \tag{1.58}$$

The final reaction $p \leftrightarrow n + e^+ + \nu_e$ is not possible, as it would violate energy conservation, which is obvious if one considers the reaction from rest frame of the proton. For most other rates, we can measure λ experimentally for the forward rate $Q > 0$, and using detailed balance to estimate the corresponding reverse rate. The conditions required for maintaining nuclear statistical equilibrium between neutrons and protons cannot be achieved experimentally, and the rate therefore must be determined theoretically. This involves evaluating several integrals, which depend on both electron and neutrino density, in addition to the temperature and scale factor. Several corrections must also be made to account for the radiative, zero-temperature, corrections, finite nucleon mass corrections, finite temperature radiative corrections, weak-magnetism, and QED plasma effects[13]. The final result mainly depends on temperature and experimentally determined mean neutron lifetime, τ_n. Since it isn't affected by the later reactions, it is sensible to just fit the result as a function of temperature and mean lifetime. In this thesis I will use the result given in appendix C of [10], which is parametrized,

$$\lambda_{n\to p} = \frac{1}{\tau_n} e^{-q_{np}/z} \sum_{i=0}^{13} a_i z^{-i} \quad , \quad 0.01 \le T/\text{MeV} \le 10 \tag{1.59}$$

$$\lambda_{p\to n} = \begin{cases} \frac{1}{\tau_n} e^{-q_{pn}\cdot z} \sum_{i=0}^{10} b_i z^{-i} & , \quad 0.1 \le T/\text{MeV} \le 10 \\ 0 & , \quad 0.01 \le T/\text{MeV} \le 0.1 \end{cases} \tag{1.60}$$

With the fitted parameters being the constants a_i and b_i as well as q_{np} and q_{pn}.

1.4 Initial conditions

1.4.1 Initial temperature

When performing BBN calculations, it is most sensible to choose an initial temperature, and from it, determine all other initial conditions. The chosen temperature

should be sufficiently high, so that all particles are in thermal equilibrium. Most BBN codes use 2.7e10 K as the initial temperature. Higher temperatures could be used, but this is unnecessary and will often lead to numerical instabilities, which I will touch upon in Chapter 2.

1.4.2 Initial time

Though none of the equations describing BBN, have any explicit time dependence, it is still nice to know the age of the universe when it takes place. This can be achieved by integrating equation (1.6), with $T = \infty$ at $t = 0$.

$$\int_0^{t_i} dt = -\int_\infty^{T_i} (24\pi G\rho_{tot})^{-1/2} \frac{\frac{d\rho_{set}(T)}{dT}}{\rho_{set}(T) + P_{set}(T)} dT \tag{1.61}$$

For high temperatures we can assume that the electrons are completely relativistic. Based on the result for neutrinos (1.22), we know that the energy of a massless fermion differs from that of a boson by a factor of 7/8. Accounting for the g factors, we get $\rho_e = 7/4\rho_\gamma$. At temperatures above 2 MeV the relativistic approximation deviates by less than 1%, see figure 1.1.

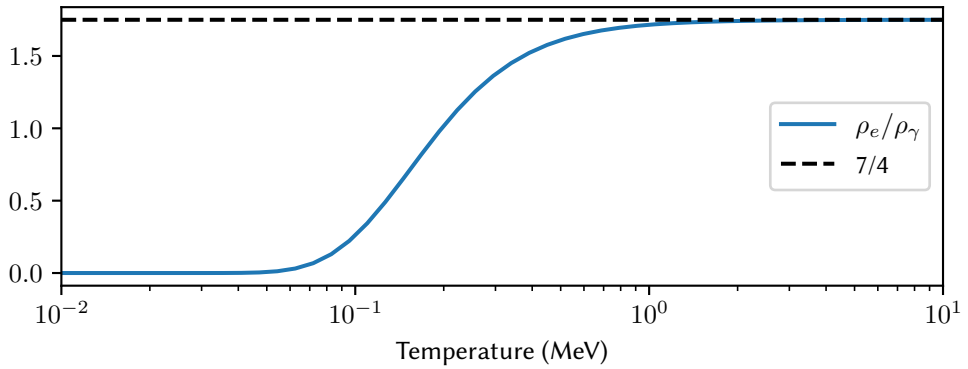

FIGURE 1.1: Exact ratio of the electron-positron energy to the photon energy.

At these temperatures we can safely ignore the baryon contribution, which combined with (1.17), allows us to calculate the non-decoupled terms.

$$\frac{\frac{d\rho_{set}(T)}{dT}}{\rho_{set}(T) + P_{set}(T)} = \frac{3}{4}\frac{1}{\rho_{set}(T)}\frac{d\rho_{set}(T)}{dT} = 3T^{-1} \tag{1.62}$$

For the total energy we simply add the contributions of all components, excluding baryons,

$$\rho_{tot} = \rho_\gamma + (2+3)\frac{7}{8}\rho_\gamma = \frac{43}{8}\rho_\gamma \tag{1.63}$$

Inserting into (1.61), we get the initial time,

$$t_i = 3(24\pi G\frac{43}{8}\frac{\pi^2}{15})^{-1/2}\int_\infty^{T_i} T^{-3}dT \tag{1.64}$$

$$t_i = \frac{3}{2}(\frac{43}{5}G\pi^3)^{-1/2}T_i^{-2} \tag{1.65}$$

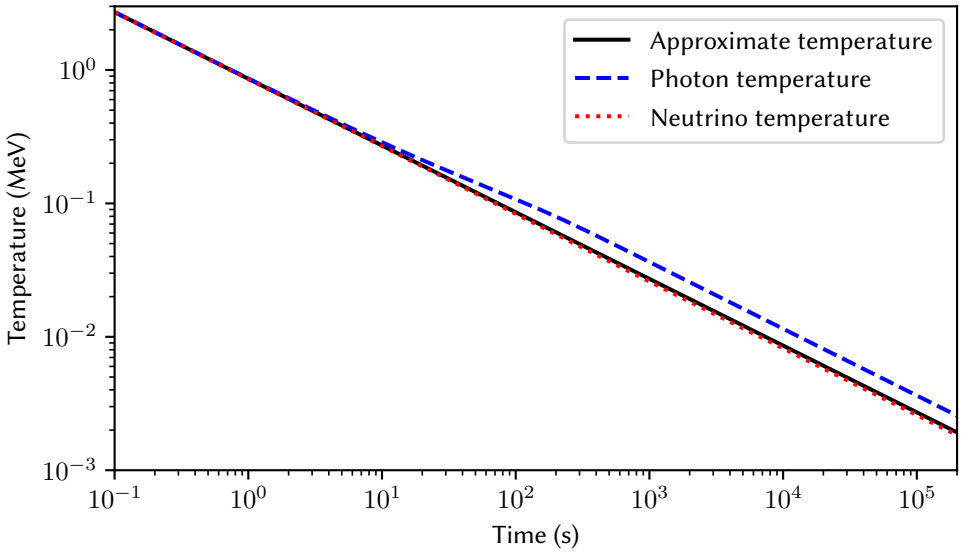

FIGURE 1.2: The temperature of photons and neutrinos during the time period of BBN, as well as the approximate temperature given by 1.65.

This relation is valid at all times before decoupling, and remains approximately true at later times, as shown on figure 1.2.

To get a sense of scale for this result we can rewrite it in units of $10^9 K$ and seconds.

$$T_9 = (43\frac{4}{3}\pi\frac{a}{c^2}G)^{-1/4}t^{-1/2} = 9.97t^{-1/2}, \tag{1.66}$$

with a being the radiation constant, related to the Stefan–Boltzmann constant by $a = \frac{4}{c}\sigma$. Using this we can justify the omission of particles heavier than electrons. The lightest of these are the muon and pion, which both have masses above 100 MeV. Significant pair creation will occur at $T_9 \geq 10^3$, corresponding to $t \approx 10^4$. As such they will have no significant impact on the initial time.

We note that (1.66) differs significantly from the expression derived by Wagoner[4],

$$T_9 = (12\pi\frac{a}{c^2}G)^{1/4}t^{-1/2} = 10.4t^{-1/2}, \tag{1.67}$$

The analytical expression is wrong, but the numerical result is correct. A simple error which probably was the result of a small mistake when transcribing the notes used for the paper. Unfortunately, this expression has been reproduced in several later BBN codes such as NUC123[7] and AlterBBN[14]. Though Kawano reproduced the equation in the documentation, in the actual NUC123 code he used the numerical result and as such the code itself had no errors. In AlterBBN they used natural units, and so couldn't use the numerical value, leading to the error affected the code. Additionally, they also confused the Stefan–Boltzmann and radiation constants leading to an additional error. Examining the code, one can see that their value is wrong by 14 orders of magnitude. Since it doesn't impact final abundances, this

error was only very recently discovered. The first correction being released in 2021 by Sharpe [16],

$$T_9 = (48\pi \frac{a_r}{c^2} G)^{-1/4} t^{-1/2} = 10.4 t^{-1/2}, \tag{1.68}$$

However this still differs from (1.66). This due to the fact that the original derivation was performed by Wagoner in 1967, a decade before the discovery of the Tau and corresponding neutrino. And though later projects correctly added the additional neutrino flavor when calculating the neutrino energy, the impact it has on the initial time had been overlooked before this thesis.

Chapter 2

BBN code

2.1 A brief history of BBN codes

The concept of Big Bang nucleosynthesis is almost as old as the Big Bang theory itself, with the with it first being proposed in the paper by Alpher, Bethe, and Gamow [2]. This early model used neutron capture and subsequent beta decay as the mechanism for BBN, though its greatest problem was the inability to explain the unusually high abundance of oxygen and carbon in the present universe. And so, it was in large part supplanted by the new theory of stellar nucleosynthesis, as the main explanation for the origin of elements.

During the next decades it became clear that stars could not be the only explanation for the present element abundances, and with the discovery of the CMB in 1965, new attention was brought to the early universe. Only a year later Peebles showed how simple BBN physics could be used to explain the high helium abundance, unaccounted for by stellar nucleosynthesis [3].

In the following years Wagoner created and refined the first proper BBN code, described in a series of defining papers[4][5][6]. With the legacy of this code still heavily influencing the way BBN calculations are performed today.

By the late 80s the Wagoner code was severely outdated. With multiple inefficiencies due to among other things, the fact that it was originally designed to run on punch cards. This inspired Lawrence Kawano to create the now ubiquitous NUC123, colloquially know as the Kawano code[7]. Which set the gold Standard for all future BBN codes.

2.1.1 Modern codes

In current day and age, there exists multiple publicly available BBN codes, and a countless number of private codes. The most well know of these are PArthENoPE, AlterBBN, and PRIMAT.

PArthENoPE[17] is a spiritual successor to NUC123, and like the works of Wagoner and Kawano PArthENoPE uses FORTRAN. It retains the same structure, and can generally be seen as a continually updated version of these earlier works, with features such as updated reaction rates and a user-friendly GUI.

PRIMAT[13] is a Mathematica code and unlike PArthENoPE and AlterBBN, it isn't directly based on the older BBN codes. The main focus of PRIMAT is improving the precision of BBN codes specifically the He4 abundance, which is mainly determined by the $p \leftrightharpoons n$ rates.

AlterBBN is written in c and based on Kawano's NUC123. It maintains the same basic structure and integration method, though it uses natural units for everything but the reaction network. However, they define energy in GeV rather than MeV. What separates AlterBBN for other codes is that as the name implies, it allows the use of alternate cosmological models and parameters. Therefore, this code is especially well suited for testing the effects these alterations have on final abundances.

2.2 Integrating the system of equations

The objective of any BBN code is to solve the system of differential equations described in chapter 1, which presents some numerical difficulties.

Most nuclear reactions have a linear or quadratic dependence on density, as well as an often exponential dependence on temperature. At high temperatures this is balanced by the corresponding reverse rate being equally high. The forward and reverse rates will only cancel at the precise abundance required by nuclear statistical equilibrium (NSE). Any slight deviation from NSE δY, will cause one rate to be slightly larger, which due to its magnitude will cause a huge increase in the derivative Y'.

Most numerical methods for solving differential equations are explicit, and in their simplest form calculate the next step by adding $\Delta Y = \Delta t \cdot Y'$. If $\Delta Y > 2\delta Y$, the system will become unstable as each step will increase the absolute value of both. To avoid this instability an explicit method will have to use a minuscule step size Δt, which in practice makes the problem unsolvable.

This and similar problems are called stiff, since they are very inflexible when faced with slight deviations from the "true" solution.

Integration methods

Wagoner and the later codes based on this work handle the stiffness by first linearizing the system, which allows integration in an implicit form:

$$\tilde{Y}_{n+1} = (1 + C\Delta t)\tilde{Y}_n \approx (1 - C\Delta t)^{-1}\tilde{Y}_n. \tag{2.1}$$

This is then followed by a traditional second order Runge-Kutta integration, with AlterBBN having options for more advanced Runge-Kutta methods.

PRIMAT on the other hand uses a first order BDF scheme for $T > 1.25\text{e}9$ K, switching to second order at lower temperatures for faster computation.

I have chosen to use an implicit Runge-Kutta method of the Radau IIA family of order 5, as implemented in SciPy. This method is perfectly suited to handle stiff problems such as the reaction network, and based on testing it is the most stable method among those available in SciPy.

2.2.1 Simplifications of the problem

Following the example of Wagoner, most BBN codes solve the background variables and abundances concurrently. This is necessary as they account for the change in baryon energy density and electron chemical potential caused by nucleosynthesis. Accounting for the baryon energy only results in a relative abundance change lower than 10^{-5} for the heavier nuclei, and even less for lighter ones. Accounting for baryons at all is questionable, and tracking the abundance of non-thermal electrons and energy changes caused by nucleosynthesis is completely unnecessary. Accordingly, the background variables can be treated as independent of the abundances.

This is beneficial, as unlike the abundances the equations governing temperature and scale factor are not stiff in the slightest. This allows faster integration, with fewer evaluations of computationally demanding terms such as the sum in electron energy density (1.34). Barring e^- e^+ annihilation, T and a follow the simple power laws $T^{-2} \propto t$ and $a^2 \propto t$, as seen on figure 1.2. This allows the use of simple linear interpolation in log space, which will have negligible impact on runtime compared to the evaluation of reaction rates.

Compared to the background parameters, evaluating reaction rates is quite simple, with the most time-consuming part being the sheer number of rates, which can be mitigated somewhat with parallelization. Here the main problem is the aforementioned stiffness, but this is also aided by precomputing the background variables, as this demonstrably improves stability.

2.3 Creating the reaction network

To create the reaction network I use pynucastro[18], which is an open source python interface designed for nuclear astrophysics. The reaction rates themselves are provided by the REACLIB database[11]. These rates are based on fits of experimental results using the following parametrization

$$\lambda = \exp\left(a_0 + \sum_{i=1}^{5} a_i T_9^{\frac{2i-5}{3}} + a_6 \log T_9 \right). \tag{2.2}$$

T9 is the temperature in 1e9 K, and the molar density must be provided in cgs units of mol/cm^3. Converting from natural units to cgs is a simple matter of multiplying by $\frac{MeV}{\hbar c}^3 \frac{1}{N_0} = 2.161\text{e}8\,\text{cm}^{-3}$, with N_0 being the Avogadro number. For some reactions such as those with powerful resonances, a rate can be comprised of multiple terms of the form given in (2.2), to allow for more accurate fit of the data.

To create the network, pynucastro must first be provided with the list of included nuclei. It has a built-in method for collecting all reactions between these nuclei which creates a library object containing the rates and their relations. This can then be used to generate a python file which takes density, temperature and abundances as inputs and returns the rhs and Jacobian. This file supports just in time compilation using the JIT module from Numba, which takes between a few seconds to a few minutes depending on the size of the network. To avoid having to compile the networks every time I modify the code, I added a method that compiles the network ahead of time using the Numba CC module.

At high temperatures heavy nuclei have extremely low abundances while greatly increase the stiffness of the system. To increase both stability and performance, it is prudent to extend the network gradually, which can be accomplished by using 3 different reaction networks.

At very high temperatures, deuterium is readily destroyed by high energy photons inhibiting the production of any subsequent nuclei. Here the simplest possible reaction network is employed, comprised of only the proton, neutron, their forward and reverse rate.

When temperatures are low enough to allow deuterium production then network is extended to include all nuclei with $A \leq 7$, see figure 2.1. This accounts for the nuclei involved in ^{4}He production and their immediate fusion products, which are also the only nuclei with observable final abundances.

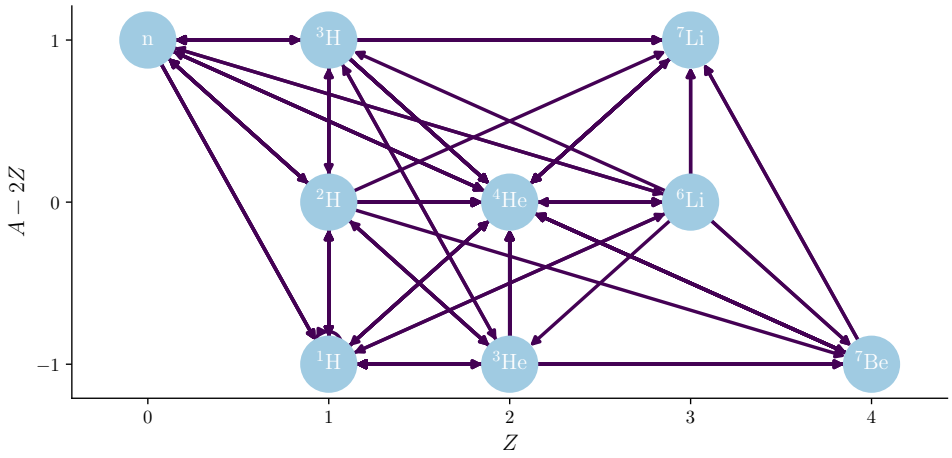

FIGURE 2.1: Reduced reaction network for calculating light element abundances at high temperatures, with arrows representing forward reaction rates.

When significant amounts of ^{4}He and heavier nuclei have formed, we switch to the full network which includes every nucleus that could possibly affect BBN, see figure 2.2. Due to the extreme temperature dependence of reactions such as triple alpha, this network is very stiff at high temperatures.

2.4 Running the code

- We use pynucastro to generate the reaction networks. This is by far the most time-consuming step, but unless we need to modify a reaction rate, we only need to do it once.
- The time evolution of background parameters is calculated and stored. To speed up subsequent calls to the background parameters, JIT is use for the interpolation function.
- Initial conditions are set based on the background parameters, with the proton and neutron abundance being determined from NSE.

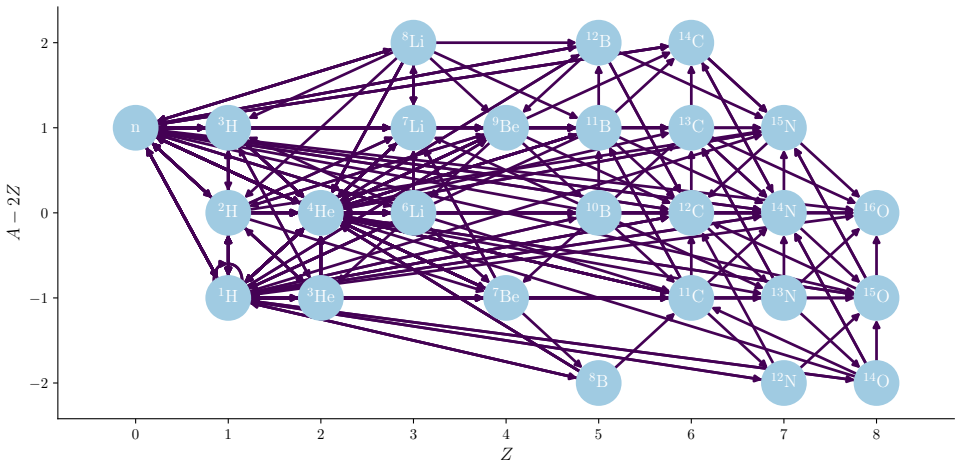

FIGURE 2.2: Full reaction network for more precise determination of heavy element abundances at intermediate to low temperatures, with arrows representing forward reaction rates.

- The first reaction network is integrated, from a specified initial time until the switch to the second network.
- Before beginning integration the second network, the initial abundance of the added nuclei is determined by requiring that the resulting RHS is 0. This minimizes the transients created as the new nuclei rapidly readjust due to the stiffness of the system.
- The second reaction network is integrated using these initial conditions, after which the same procedure is used for the third network.
- Barring the addition of additional reaction networks, we get the final abundances, as well as their evolution over time.

Chapter 3

Results

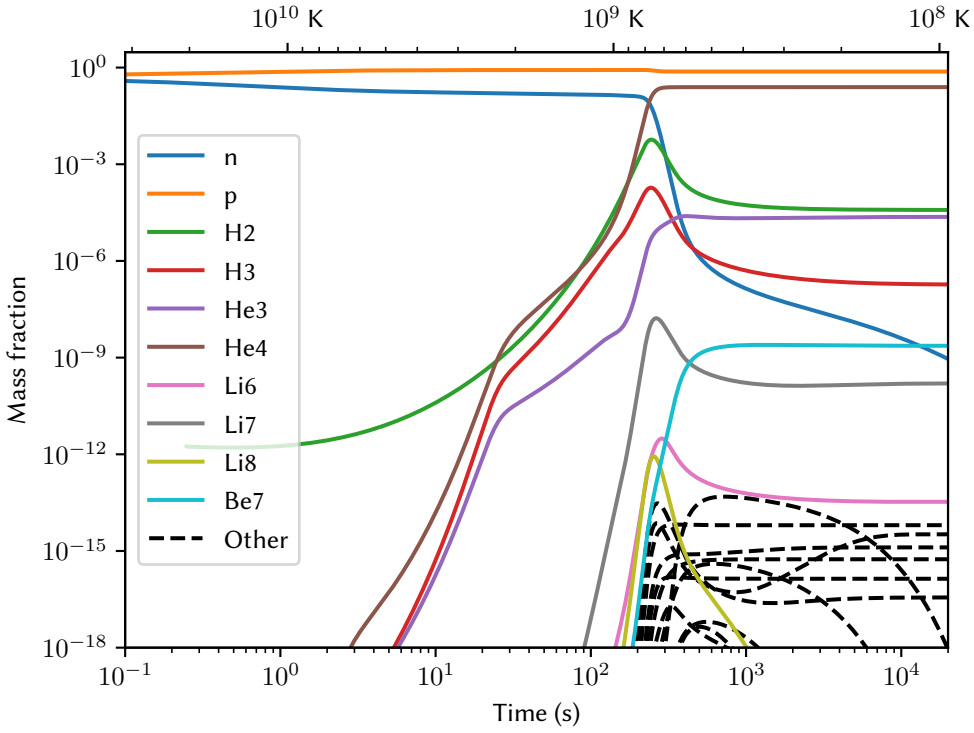

Figure 3.1: Time evolution of light nuclei abundance during BNN, with mass fraction technically being the close approximation $X_i = Y_i A_i$. .

Running the code creates a complete overview of abundance evolution as shown on figure 3.1. As expected neutrons protons and deuterium remain in equilibrium for the first few seconds. As the temperature decreases, deuterium abundances slowly increase quickly followed by tritium and both helium isotopes. Here the dominant nuclear reactions are neutron captures creating tritium, and converting ^{3}He to ^{4}He, which continues until around 230 seconds. At this point the rate of deuterium

creation is finally great enough to have a significant impact on neutron abundance, which until then had remained almost unchanged since the $p \leftrightarrow n$ rates fell out of equilibrium. This leads to a rapid drop in neutron abundance creating a bottleneck on the production of deuterium and tritium, which in turn slows down and eventually stops the production of ^{3}He and ^{4}He. Without these light nuclei lithium abundances also drop, as reactions such as $^4\text{He} + {}^3\text{H} \rightarrow {}^7\text{Li}$ become outmatched by the proton captures $^7\text{Li} + \text{p} \rightarrow 2{}^4\text{He}$ and $^6\text{Li} + \text{p} \rightarrow {}^7\text{Be}$. Conversely, Beryllium 7 is primarily destroyed via neutron capture $^7\text{Be} + \text{n} \rightarrow {}^7\text{Li} + \text{p}$, and therefore sees a rapid increase in abundance immediately after the drop in neutrons.

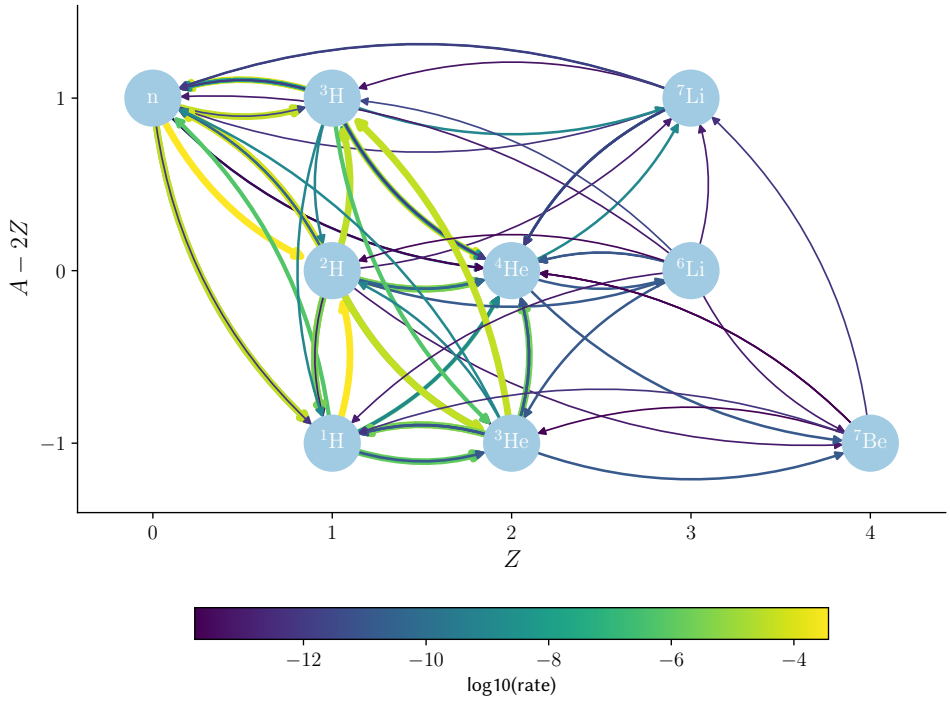

FIGURE 3.2: Reaction rates 5 minutes after Big Bang at 7.6e8 K. Only including rates within 10 orders of magnitude of strongest..

The relations of these reactions are illustrated in figure 3.2. This snapshot is taken immediately after the aforementioned drop in neutron abundance with $Y_n = 0.2\%$. Despite this $n + p \rightarrow d$ is still the strongest reaction, followed by reactions creating ^{3}He and ^{3}H.

Equal d and n mass fraction The

3.0.1 Dominant reactions

3.1 Precision

Throughout the code there are several numerical

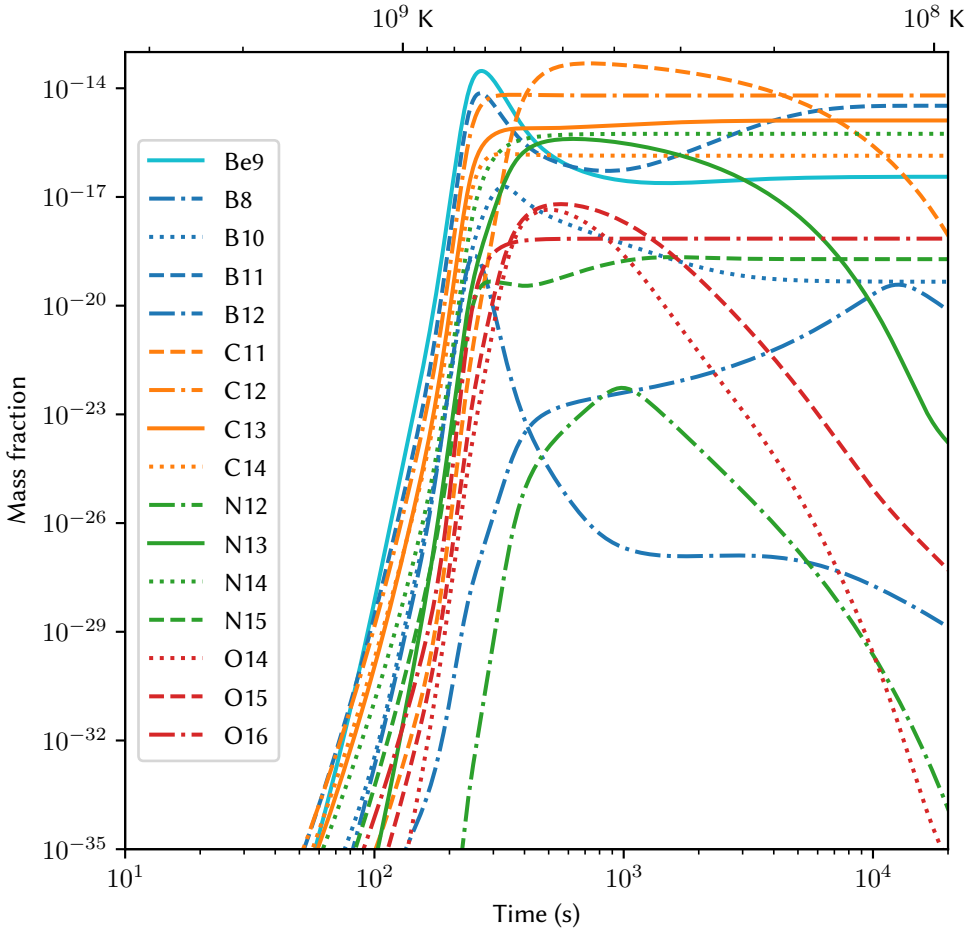

FIGURE 3.3: Time evolution of heavy nuclei abundance during BNN, with mass fraction technically being the close approximation $X_i = Y_i A_i$..

3.1.1 Electron energy

3.1.2 Tolerances

3.1.3 Interpolation

3.1.4 Initial time

3.1.5

3.2 Comparison with AlterBBN

3.3 Final abundances

3.4 Nuclear solutions to the Lithium problem?

Bibliography

[1] S. Chandrasekhar. *An Introduction to the Study of Stellar Structure*. First Edition. THE UNIVERSITY OF CHICAGO PRESS, 1939.

[2] R. A. Alpher, H. Bethe, and G. Gamow. "The Origin of Chemical Elements". In: *Phys. Rev.* 73 (7 Apr. 1948), pp. 803–804.

[3] P. J. E. Peebles. "Primordial Helium Abundance and the Primordial Fireball. II". In: *The Astrophysical Journal* 146 (Nov. 1966), p. 542.

[4] Robert V. Wagoner, William A. Fowler, and F. Hoyle. "On the Synthesis of Elements at Very High Temperatures". In: *The Astrophysical Journal* 148 (Apr. 1967), p. 3.

[5] Robert V. Wagoner. "Synthesis of the Elements Within Objects Exploding from Very High Temperatures". In: *The Astrophysical Journal Supplement* 18 (June 1969), p. 247.

[6] Robert Wagoner. "Big-Bang Nucleosynthesis Revisited". In: *The Astrophysical Journal* 179 (Dec. 1972), pp. 343–360.

[7] Lawrence Kawano. "Let's go: Early universe. 2. Primordial nucleosynthesis: The Computer way". In: (Jan. 1992).

[8] E. Kolb and M. Turner. *The Early Universe*. Frontiers in physics. Avalon Publishing, 1994.

[9] B. Ryden. *Introduction to cosmology*. Second Edition. Cambridge University Press, 2002.

[10] P D Serpico et al. "Nuclear reaction network for primordial nucleosynthesis: a detailed analysis of rates, uncertainties and light nuclei yields". In: *Journal of Cosmology and Astroparticle Physics* 2004.12 (Dec. 2004), pp. 010–010.

[11] Richard H. Cyburt et al. "The JINA REACLIB Database: Its Recent Updates and Impact on Type-I X-ray Bursts". In: *The Astrophysical Journal Supplement* 189.1 (July 2010), pp. 240–252.

[12] Pablo F. de Salas and Sergio Pastor. "Relic neutrino decoupling with flavour oscillations revisited". In: *Journal of Cosmology and Astroparticle Physics* 2016.07 (July 2016), pp. 051–051.

[13] Cyril Pitrou, Alain Coc, Jean-Philippe Uzan, and Elisabeth Vangioni. "Precision big bang nucleosynthesis with improved Helium-4 predictions". In: *Submitted to Phys. Rept.* (2018).

[14] A. Arbey, J. Auffinger, K. P. Hickerson, and E. S. Jenssen. *AlterBBN v2: A public code for calculating Big-Bang nucleosynthesis constraints in alternative cosmologies*. 2019.

[15] Planck Collaboration et al. "Planck 2018 results. VI. Cosmological parameters". In: *Astronomy and Astrophysics* 641, A6 (Sept. 2020), A6.

[16] Charlie Sharpe, Geraint F. Lewis, and Luke A. Barnes. *Big Bang Nucleosynthesis Initial Conditions: Revisiting Wagoner et al. (1967)*. 2021.

[17] S. Gariazzo, P. F. de Salas, O. Pisanti, and R. Consiglio. "PArthENoPE revolutions". In: *Computer Physics Communications* 271 (Feb. 2022), p. 108205.

[18] Alexander I. Smith et al. "pynucastro: A Python Library for Nuclear Astrophysics". In: *The Astrophysical Journal* 947.2 (Apr. 2023), p. 65.

[19] *NIST Digital Library of Mathematical Functions*. `https://dlmf.nist.gov/`, Release 1.1.11 of 2023-09-15. F. W. J. Olver, A. B. Olde Daalhuis, D. W. Lozier, B. I. Schneider, R. F. Boisvert, C. W. Clark, B. R. Miller, B. V. Saunders, H. S. Cohl, and M. A. McClain, eds.